24th International Conference on Renewable Energies and Power Quality (ICREPQ'26)
Santander (Spain), 10th to 12th June 2026
ISBN-13: 978-84-09-82044-3

Distance Protection in IBR-Rich Systems Using an Incremental Time-Domain Algorithm

A. Blazquez, E. Torres, D.M. Larruskain, I. Santamarina, A. Iturregi, P. Eguia

Department of Electrical Engineering, School of Engineering in Bilbao, University of the Basque Country EHU
Plaza Ingeniero Torres Quevedo 1, 48013 Bilbao, Spain
aitor.blazquez@ehu.eus

Abstract. Currently conventional protection relays may operate unreliably under the reduced inertia conditions and high levels of inverter based resources that characterise modern power systems. The literature consistently shows that existing algorithms and protection systems exhibit vulnerabilities: inappropriate tripping, causing unnecessary interruptions in energy delivery, or undetected faults due to the inherent limitations of traditional relay logic and the limited suitability of phasor-based estimation for representing fast, non-sinusoidal transient behaviour. The paper examines a time-domain incremental approach to enhance the reliability of distance protection functions operating in environments with substantial IBR penetration. Building on the limitations of conventional phasor-based schemes, the work assesses how incremental quantity processing can better characterise the fast, non-sinusoidal transients produced during faults in converter dominated systems. Methodological approach is presented, with the objective of mitigating the impaired impedance-based response observed under inverter-based system conditions, ensuring stable and reliable distance protection performance in several study cases.

Key words. Distance Protection, Incremental Quantity, Inverter Based Resources, Time-Domain.

1. Introduction

Modern power systems with high penetration levels of inverter based resources (IBRs) exhibit fault behaviours shaped by converter controls rather than by synchronous machine dynamics, producing responses for which conventional relays were not originally designed. As a result, traditional protection elements may misclassify disturbances, either triggering unnecessary trips or failing to detect genuine faults [1-3]. This arises from the mismatch between legacy relay logic, developed for predictable electromechanical systems, and the rapidly evolving, non-standard current waveforms encountered in IBR dominated networks, reducing the robustness of established protection practices under contemporary conditions.

Distance protection is particularly affected, as the fault currents supplied by converters often lack the magnitude and stability required for accurate impedance-based decision making. Control driven current limiting and reduced source contribution can distort the apparent impedance, leading to classical mal-reach behaviours and undermining dependability [2-5]. These effects intensify as the share of IBRs increases, highlighting the diminishing suitability of conventional distance schemes for future power system architectures.

Conventional protection relies on phasor quantities, assuming that voltages and currents can be represented by their fundamental components and that system behaviour remains effectively steady over a cycle [6]. These assumptions become increasingly fragile as operating conditions evolve more rapidly, reducing the reliability of phasor estimates. These schemes must wait at least one full cycle to derive accurate post-fault phasors, so their reaction time is inherently limited, restricting the speed with which a trip can be issued [6-7].

Fast fault clearance, however, is essential for maintaining dynamic system security. Delays in isolating a disturbance may compromise transient stability and, in extreme scenarios, contribute to widespread service disruption. This challenge is even more pronounced in power systems with high penetrations of IBRs, where reduced inertia and limited fault current reduce the system's tolerance to disturbances. Under these circumstances, even small improvements in operating speed can significantly enhance stability margins, highlighting the importance of protection methods capable of delivering rapid and dependable action [6].

In view of these challenges, one promising direction for the development of next generation protection schemes is to minimise reliance on detailed assumptions about the behaviour of generation sources and, instead, act before the sources have time to influence the system's response. This has led to growing interest in protection techniques that operate directly in the time-domain, analysing the earliest stages of the fault transient where the waveform carries rich diagnostic information. Methods based on incremental quantities (IQ), which extract dynamic changes in voltage and current rather than relying on their steady-state phasor representations, offer a particularly attractive pathway in this regard [6]. By exploiting these rapidly evolving time-domain features, prior to significant converter control action, protection strategies can retain selectivity and reliability even in networks dominated by IBRs.

Protection schemes based on IQ have been proposed in the literature, such as IQ based directional protection [8] and distance protection algorithm for series compensated lines [9]. In [10] a novel IQ based distance protection algorithm is proposed which analyses the impact of the fault angle, fault resistance and line transposition schemes. [9-10] are formulated for conventional synchronous generation and therefore do not account for the nonlinear controls, limited fault-current capability, or dynamic behaviour characteristic of IBRs. The influence of grid-forming inverters on the performance of protection schemes based on IQ is analysed in [11], but the study relies on a single idealized GFM model that does not reflect the heterogeneous controls and nonlinear current-limiting behaviour of Type-4 wind turbines, while its simplified single-source topology neglects the multi-unit interactions, unequal fault-current contributions and collective transients characteristic of real wind plants.

The paper presents a time-domain IQ framework. After a concise introduction to how IQ isolate the earliest transient components, the paper proposes an IQ distance protection scheme tailored to the challenges posed by IBRs. Its performance is examined through a detailed study case involving a Type 4 wind farm connected to a high-voltage transmission system, where several fault types and locations are analysed to assess sensitivity, selectivity and reliability. Finally, main conclusions highlight the improved robustness and achieved consistency.

2. Incremental Quantities

IQs are defined by comparing instantaneous electrical values at two distinct moments separated by a time interval, typically an integer multiple of the system's fundamental period [6]. Under ideal circumstances these differences should vanish, while during normal operation they remain small, making them useful indicators of abnormal behaviour. As the IQ values are inherently low but non-zero, appropriate safety margins must be incorporated to prevent erroneous detection [10].

Using the superposition principle, a faulted power system can be represented by two complementary networks: the prefault network and the pure fault network. The former reflects the steady state operating conditions prior to the disturbance, whereas the latter contains only the Thévenin voltage source, whose magnitude is equal to the negative prefault voltage at the fault location. Before the disturbance, voltages and currents are zero in the pure fault network. Once the fault occurs, it transitions through a transient regime before reaching a new steady state. IQ remain valid throughout both regimes [7].

Analysing the two networks independently allows separation of the load related components of voltages and currents from those generated specifically by the fault. The complete solution at any location is obtained by the sum of these two contributions. This decomposition makes it possible to identify replica, or delta, signals, which represent changes in voltage and current arising solely from the disturbance. These Δv and Δi values form the basis for protection algorithms and the definition of associated operating thresholds [6]. IQ are computed using instantaneous measurements according to (1)[12].

$$\Delta s(t) = s(t) - s(t - pT) \tag{1}$$

where Δs is the instantaneous IQ, s is the measured instantaneous value, t is the present time, T is the fundamental period of the measured parameter, and p specifies how many cycles in the past are referenced, typically, p=1 and p=2 are shown in the literature. Besides, a second order expression is proposed in [13], where the instantaneous values are calculated with (2).

$$\Delta s(t) = s(t) - 2s(t - T) + s(t - 2T) \tag{2}$$

Measured fault signals consist of the sum of prefault and fault generated components. Relays obtain incremental values by subtracting the extrapolated prefault estimates from the instantaneous quantities observed at the relay terminals. This extrapolation is reliable only for a short duration, typically a few tens of milliseconds, before source dynamics render the prefault prediction inaccurate.

3. Incremental Quantity Based Distance Protection

Distance protection determines the location of a fault by estimating the apparent impedance between the relay and the fault, issuing a trip when this impedance falls below a preset reach. This way, distance elements include a predefined reach point and are designed to operate exclusively for faults located within this protected region. The operating signal is explicitly obtained as the instantaneous voltage change at the reach point, calculated using the incremental voltage, the incremental replica current, and the line RL parameters [14-15].

Fig. 1 shows the flowchart of the IQ based distance protection algorithm, with the measured instantaneous phase currents and voltages as inputs. The process begins by loading the line parameters and zone settings required for impedance-based fault detection. The relay then continuously measures the three-phase voltages (Vabc) and currents (Iabc), applying filtering and prefault memory logic to stabilize the calculations during transient conditions.

Next, the algorithm computes the incremental voltage and current as shown in (1), and uses them to derive the incremental impedance (ΔZ) for each fault loop. Directional and polarity checks are then applied to confirm the fault direction and ensure correct discrimination between forward and reverse conditions [9]. The resulting ΔZ is compared against the predefined thresholds for protection zones 1, 2 and 3, if the value falls within a zone boundary, the relay issues the corresponding trip command.

This tripping logic is based on the premise that the prefault voltage provides the maximum expected value of the voltage change at the reach point. Consequently, when the instantaneous voltage change exceeds the prefault value, the fault must lie within the selected reach setting [15]. In this scheme, the prefault voltage at the reach point acts as the restraining signal, enhancing both sensitivity and security [14].

To ensure comprehensive coverage of all fault types, the relay evaluates six independent measurement loops, three phase-to-ground and three phase-to-phase, computing the reach-point voltage using both incremental quantities and one-cycle-old steady-state values. This implementation explicitly uses the transmission line RL parameters to model the expected behaviour of the voltage change, thereby improving the accuracy of the reach calculation [14]. The element provides individual tripping outputs, along with configurable settings such as phase and ground reach values and the IQ operating threshold.

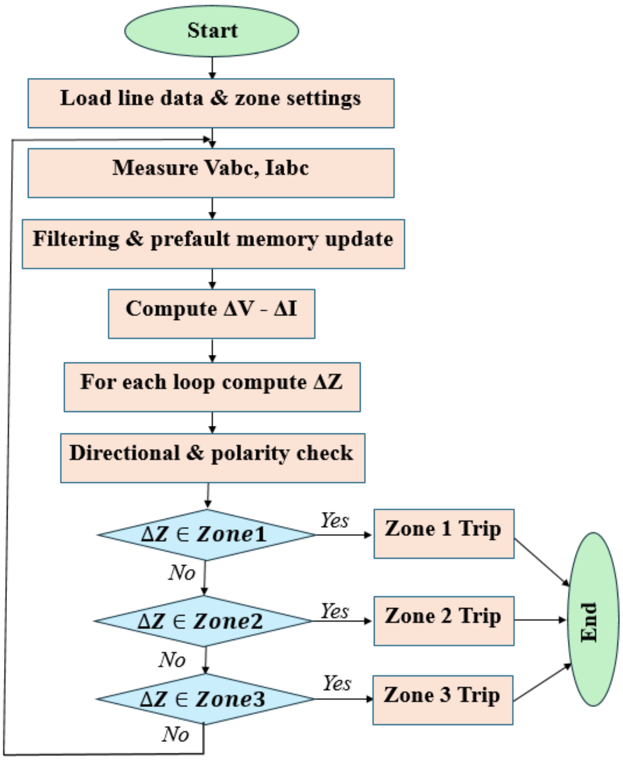

Fig. 1. IQ based distance protection flowchart.

From an implementation perspective, the scheme must operate within strict computational constraints, as the incremental quantities and directional checks must be evaluated every sampling interval without introducing processing delays. This requires efficient filtering, numerical stability in the ΔV/ΔI calculations, and careful handling of noise-induced distortions, particularly under low-voltage or high-infeed conditions. Furthermore, the use of prefault memory imposes requirements on buffer management and synchronization, ensuring that stored quantities remain valid and unaffected by transient events.

4. Study case

A. Network model

The network model implemented in this study is shown in Fig. 2 and represents a Type 4 wind farm with five wind turbines, which is connected to a 120 kV power system. Short-circuit strength value of 100 MVA is considered to model the upstream network which correspond to SCR value of 9.

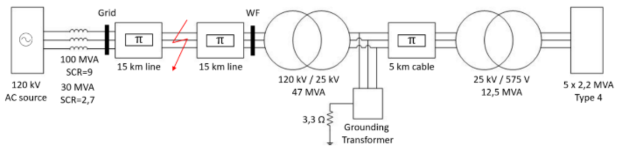

Fig. 2. Network model.

Table I shows the parameters of the AC source and the equivalent grid impedance.

Table I. – AC grid.

	SYMBOL	VALUE
AC Three Phase Source	S	100 MVA
	U_{AC}	120 kV
	f	50 Hz
AC impedance	R_1	0,1 Ω
	L_1	1 H
	R_0	0,3 Ω
	L_0	3 H

The windfarm is connected to the system through a 30 km overhead transmission line and a 120 kV/25 kV transformer, whose main data are shown in Table II.

Table II. – Line and transformer parameters.

	SYMBOL	VALUE
30 km line	R_1	0,176 Ω/km
	L_1	1,57e-3 H/km
	C_1	0,0127e-6 F/km
	R_0	0,42 Ω/km
	L_0	3,82e-3 H/km
	C_0	0,007e-6 F/km
HV-MV transformer	V_1	120 kV
	V_2	25 kV
	S	47 MVA
	Ucc	16%

The wind farm is represented by an equivalent model, consisting of a 5 km underground cable and an equivalent 25 kV/575 V turbine transformer rated at 12.5 MVA. The technical characteristics of these components are provided in Table III and IV. The medium voltage network is earthed through a grounding transformer with a 3.3 Ω resistor, ensuring controlled fault current levels.

Table III. – Cable parameters.

5 km MV cable	R_1	0,1153 Ω/km
	L_1	1,05e-3 H/km
	C_1	11,33e-9 F/km
	R_0	0,413 Ω/km
	L_0	3,32e-3 H/km
	C_0	5,01e-9 F/km

Table IV. – MV-LV transformer parameters.

MV-LV transformer	V_1	25 kV
	V_2	575 V
	S	12,5 MVA

The five wind turbines are modelled collectively using an equivalent Type 4 wind turbine generator (WTG) with a total capacity of 5 × 2.2 MVA, as summarised in Table V. Type 4 machines employ a full-scale power conversion system based on a back-to-back voltage source converter arrangement, comprising a machine-side converter and a grid-side converter, whose control have been also modelled in order to obtain the response of the windfarm under different control strategies and LVRT grid code requirements.

Table V. – Wind turbine parameters.

Type 4 WTG	P_{rated}	5*2 MW
	S_{rated}	5*2.2 MVA
	U_{dc}	1100 V

B. Fault case

A solid CG phase-to-ground fault is applied 18 km from the measuring point at t = 4 s. At fault inception, phase voltages become unbalanced with a voltage dip on the faulted phase, followed by partial recovery under converter control, as shown in Fig. 3. Following the fault, the converter enters LVRT mode, injecting reactive current and enforcing current limits and the system then settles into an unbalanced steady-state condition as the wind turbine's control restricts its fault-current contribution, Fig. 4.

Fig. 5 depicts the incremental voltage behaviour. Before the fault, the incremental quantities remain essentially zero, as parameters are steady and no abrupt disturbances are present in the system. At the fault inception, the incremental voltage exhibits a sharp oscillatory burst produced by the sudden collapse of the phase voltage and the associated travelling-wave components arriving at the relay location. Incremental voltage decays rapidly as the post-fault regime becomes established. This clear transition from near-zero prefault values to a well-defined transient response enables the distance-protection algorithm to accurately identify the disturbance onset. The IQ algorithm issues a trip within approximately 10 ms after fault inception, demonstrating its capability for fast fault detection, as it relies on the early transient components of the signals rather than waiting for steady-state phasor estimation.

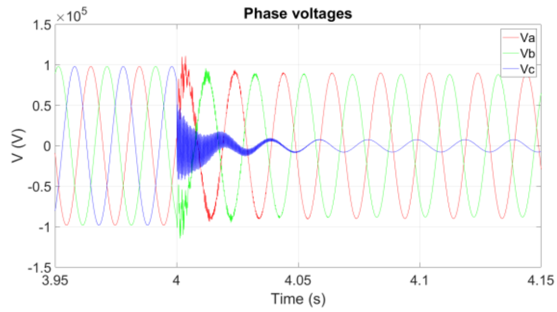

Fig. 3. Phase voltages.

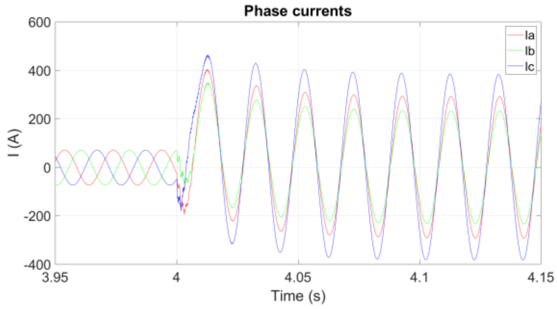

Fig. 4. Phase currents.

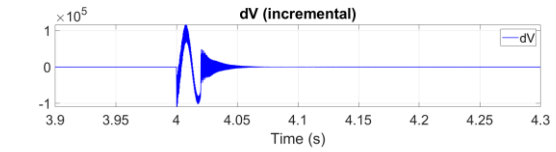

Fig. 5. Evolution of IQ under fault condition.

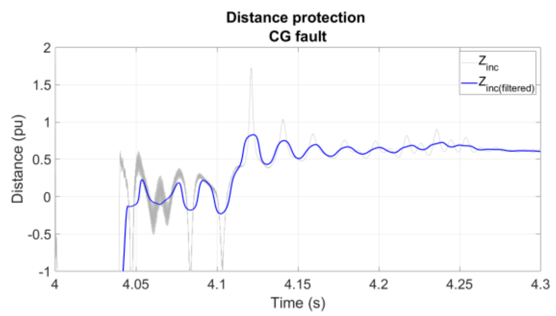

Fig. 6. Dynamic evolution of the apparent impedance.

Fig. 6 illustrates the dynamic evolution of the apparent impedance estimated by the algorithm. At the pre-fault stage, the measured incremental voltage and current are near zero, resulting in an ill-defined or noisy impedance estimate. When the fault is initiated, incremental quantities exhibit transient behavior due to the sudden change in system conditions, causing significant oscillations in the calculated impedance. As the fault develops, the algorithm begins to converge toward a steady-state estimate of the fault loop impedance. The transient spikes and dips observed in the curve are characteristic of IQ-based methods, which emphasize changes in signals rather than absolute values. This method is particularly sensitive to high-frequency components and system dynamics, including DC offsets and traveling waves. The damping observed reflects the filtering and estimation process inherent in the proposed algorithm. The calculated fault location is 62.75%, which corresponds to an absolute error of 2.75%, this represents an absolute deviation of 825 m.

C. Performance analysis of IQ methods

Three methods for calculating incremental magnitudes have been compared, corresponding to different formulations used in the literature [14,15]:

- m1, one-cycle delay, according to (1).
- m2, two-cycle delay, according to (1).
- m3, second-order operator, according to (2).

The nomenclature to indicate the Fault Type in order to maintain Tables compact is the following:

- PG, Single-phase-to-ground fault.
- PP, Phase-to-phase fault.
- PPG, Double-phase-to-ground fault.
- PPP, Three-phase fault.

Single-phase-to-ground fault category exhibits the highest divergence among the analyzed methods. Method m1 proves to be the most robust and reliable option maintaining high analytical consistency across all fault loops with an average error of 2.79%, as shown in Table VI. Fig. 7 depicts the estimation error for different fault locations, where the error increases with both the distance and the fault resistance. Method m2 exhibits a comparable performance with an error of 3.27%, although it presents slight degradation and under-reach tendencies in specific phases. The most critical finding corresponds to method m3, which reveals a severe vulnerability, showing a significantly higher error of 8.72%. Despite operating acceptably for BG faults, it introduces massive under-reach in AG and CG loops. See Fig. 8 to observe this last case. This blind spot reduces the reliability of the m3 operator for comprehensive single-phase protection.

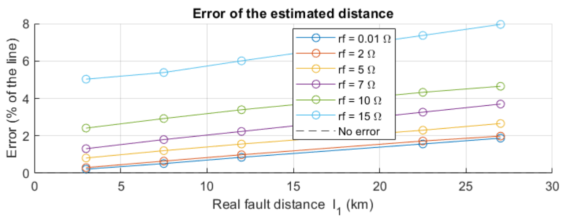

Fig. 7. BG fault, estimated error using m1.

Phase-to-phase faults display the most homogeneous and predictable behavior. All three operators show high mutual consistency and uniform over-reach tendencies. Methods m1 and m2 track the fault characteristics analogously and stably. Although method m3 registers subtly lower average deviations in this category, 4.16% compared to 5.22% for m1 and 4.65% for m2, as shown in Table VI, it introduces minor non-expected anomalies in its trends, whereas m1 ensures a completely standard and theoretical response.

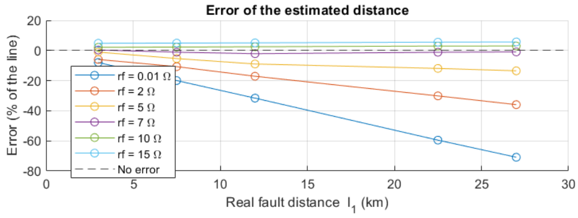

Fig. 8. CG fault, estimated error using m3.

In double-phase-to-ground fault scenarios, the impact of the chosen incremental operator is practically negligible. All three methods produce nearly identical error profiles across all simulations, with errors between 15.78% and 16.96% in Table VI. This technical uniformity demonstrates that the estimation accuracy in these complex faults is conditioned by the network physics and the current injection dynamics of the IBRs, rather than the particular mathematical formulation of the incremental method.

For three-phase faults, methods m1 and m2 exhibit superior accuracy, bounding error margins more effectively (4.56% and 4.22%, respectively, in Table VI) than method m3 (5.43%). Furthermore, all three methods successfully ratify the symmetrical and balanced nature of the short circuit, offering identical results regardless of the phase combination selected in the calculation for the incremental quantities.

Table VI. – Calculated error for different IQ methods and fault types.

	m1	m2	m3
PG	2.79	3.27	8.72
PP	5.22	4.65	4.16
PPG	16.96	16.74	15.78
PPP	4.56	4.22	5.43

Based on this comparative analysis, method m1 is selected as the definitive operator for the distance protection scheme. Method m3 is entirely discarded due to its unacceptable degradation in single-phase loops. Between m1 and m2, the former is preferred because it offers the greatest robustness against single-phase faults, which are the most frequent events in real power grids, while maintaining the simplest formulation with a single-cycle delay window.

D. Impact of fault resistance and location

The effect of fault resistance (r_f) and location (l_1) on estimation accuracy is evaluated across all fault families, considering the m1 method. Results are summarized in Table VII, which shows the calculated error for different r_f values and fault types and Table VIII that shows the calculated error for different fault types and locations.

For single-phase-to-ground faults there is a particular trend regarding r_f, the calculated error begins with a value of 2.97% at bolted conditions, decreases to a minimum of 0.94% at 2 Ω, and then experiences a moderate increase, going up to 6.13%, when the resistance reaches 15 Ω.

Regarding the dependency on distance l_1, Table VIII illustrates a gradual but steady increase, going from an error of 1.75% at 3 km to 3.84% at the end of the line (27 km).

Phase-to-phase faults again display the most predictable and uniform behavior. As observed in Table VII, the error increases strictly monotonically with r_f, starting from just 1.86% and reaching a maximum error of 12.39% at the highest tested resistance. On the other hand, Table VIII confirms that this fault family is practically independet of l_1, keeping errors bounded between 3.64% and 6.97% across all distances. This monotonic, resistance-driven over-reach is a well-known characteristic of reactance-based estimators and remains consistent across all three phase-to-phase loops.

Double-phase-to-ground faults tend to be the most sensitive to fault +resistance r_f. Table VII highlights an abrupt error growth, starting from a low value of 2.04% at bolted faults, the error reaches almost 40% at 15 Ω (37.17%). In contrast, the effect of location has a secondary impact. Table VIII reveals that for this group, the error is quite high and constant.

For three-phase faults, errors are generally low and stable. According to Table VII, the error experiences an initial drop from 4.19% under bolted conditions to just 0.58% at 2 Ω, before rising moderately to 11.66% at 15 Ω. Regarding distance, Table VIII shows a very moderate increase in error, going from 3.44% at 3 km to 5.75% at 27 km, which is consistent with the behavior reported in comparable sequence-based studies.

Table VII. – Calculated error for different r_f values and fault types.

	0 Ω	2 Ω	5 Ω	7 Ω	10 Ω	15 Ω
PG	2,97	0,94	1,23	2,18	3,29	6,13
PP	1,86	2,59	3,49	4,42	6,58	12,39
PPG	2,04	6,43	13,19	18,05	24,87	37,17
PPP	4,19	0,58	1,88	3,33	5,71	11,66

Table VIII. – Calculated error for different fault types and locations.

	3 km	7.5 km	12 km	22.5 km	27 km
PG	1,75	2,22	2,63	3,5	3,84
PP	3,64	4,27	4,88	6,34	6,97
PPG	17,19	16,69	16,54	17	17,37
PPP	3,44	3,92	4,37	5,32	5,75

As detailed in Tables VII and VIII, the methods exhibit comparable trends for both parameters. In summary, as evidenced by both tables, the algorithm maintains reliable accuracy across the full parameter range for single-phase, phase-to-phase, and three-phase faults, with errors generally remaining low under realistic resistance levels. However, the high values recorded in the double-phase-to-ground row of Table VII make it clear that double-phase-to-ground faults represent the practical accuracy boundary of the method, where fault resistance limits the achievable precision, regardless of the chosen operator.

5. Conclusions

This paper deals with a time-domain incremental method for distance protection operating in systems with high levels of IBR penetration. The analysis performed of a system connected to a Type 4 wind farm shows that the IQ algorithm, particularly when implementing the selected m1 operator, provides a reliable response for all fault scenarios considered. Fault detection occurs extremely fast, driven primarily by measurement dynamics and lightweight processing. Across a range of fault types, resistances, and locations, the method has consistently identified the faults correctly, with the calculated apparent-impedance error remaining low in most cases. The smallest deviations are observed under solid or low-resistance faults, confirming the expected robustness of IQ when the fault current variations are significant and well-defined. Moderate increases in error appeared under high-resistance faults, with the notable exception of double-phase-to-ground faults, which represent the practical accuracy boundary where errors rise more steeply. Even in these situations, the algorithm maintains a sufficiently stable behaviour to support fast protection schemes.

The comparative assessment of the incremental operators was carried out to observe different results of the algorithm. Method m1 was selected due to its superior analytical consistency in single-phase loops and its structural simplicity, while method m3 was discarded due to its unacceptable under-reach vulnerabilities in single-phase faults. Furthermore, the parametric analysis quantified the exact impact of network physics, confirming that single-phase, phase-to-phase, and three-phase faults maintain tightly bounded errors across varying distances and resistances. However, double-phase-to-ground loops face a severe accuracy limitation, reaching an error of nearly 40% at 15 Ω, probably driven by the interaction with IBR current injection dynamics.

The stable and predictable behaviour observed across all scenarios suggests that the algorithm using the m1 formulation maintains reliable operating characteristics within the evaluated range. Overall, the results indicate that the proposed approach is suitable for accurate fault characterization under typical conditions and performs within expected margins when subjected to increased fault resistance for IBR dominated systems. These findings support the viability of the method as a basis for further development and more comprehensive validation in future work. Additional studies will analyze how different negative-sequence current control strategies influence the response of the algorithm. Future work will include real-time simulations of the wind farm connected to grids with different strength conditions.

Acknowledgement

This work has been funded by the Basque Government via RESINET+ project grant (KK-2025-00100) and GISEL Research Group grant (IT1799-26).

References

[1] J. Till and Y. Liu, “A Review of Distance and Overcurrent Protection Considering Increased Inverter-Based Resources” 2023 Industry Conference, April 18-19, Tennessee.

[2] A. Haddadi, E. Farantatos, I. Kocar, and U. Karaagac, “Impact of Inverter Based Resources on System Protection,” Energies, vol. 14, no. 4, p. 1050, Feb. 2021. doi.org/10.3390/en14041050.

[3] R. Cimadevilla, A. Castañón, P. Eguia, E. Torres and A. Blazquez, "Abnormal fault patterns in the presence of inverter based generation and their effect on line protection," *19th IET Conference on Developments in Power System Protection (DPSP Europe 2025)*, Bilbao, Spain, 2025, pp. 246-254, doi: 10.1049/icp.2025.1077.

[4] M.M. Mobashsher, A.A. Abdoos, S.M. Hosseini, S.M. Hashemi, M. Sanaye-Pasand, “A new fault type classification method in the presence of inverter-based resources” International Journal of Electrical Power & Energy Systems, vol. 147, 2023, 108793, https://doi.org/10.1016/j.ijepes.2022.108793.

[5] N. M. Varghese and M. K. Jena, "Reconceptualizing the Transmission Line Protection From the Perspective of IBR-Dominated Grid," in IEEE Access, vol. 12, pp. 195065-195075, 2024, doi: 10.1109/ACCESS.2024.3520312

[6] E.O. Schweitzer, B. Kasztenny, A. Guzmán, V. Skendzic, and M.V. Mynam, “Speed of line protection-can we break free of phasor limitations?” SEL, Atlanta, Georgia, Tech. Rep., Aug. 2015.

[7] E. Schweitzer, B. Kasztenny, M. Mynam, “Performance of time-domain line protection elements on real-world faults” pp. 1–17.

[8] J. Vermunicht, W. Leterme, D. Van Hertem, “Analysing the performance of incremental quantity based directional time-domain protection near HVAC cables and VSC HVDC converters”, Electric Power Systems Research, vol. 223, 2023, 109599, https://doi.org/10.1016/j.epsr.2023.109599.

[9] T. Hoq, J. Wang, N. Taylor, “An Incremental Quantity Based Distance Protection With Capacitor Voltage Estimation for Series Compensated Transmission Lines”, IEEE Access, Vol. 9, 2021, DOI 10.1109/ACCESS.2021.3134558.

[10] Y. Chen, M. Wen, Z. Wang, X. Yin, “A novel instantaneous value based incremental quantities distance protection for AC transmission lines” Electrical Power and Energy Systems, vol. 135, 2022, 107385, https://doi.org/10.1016/j.ijepes.2021.107385.

[11] H. Johansson, Q. Xing, N. Taylor and X. Wang, "Incremental quantities protection schemes with grid-forming inverters," 19th IET Conference on Developments in Power System Protection (DPSP Europe 2025), Bilbao, Spain, 2025, pp. 277-289, doi: 10.1049/icp.2025.1081.

[12] H. Johansson, Q. Xing, N. Taylor and X. Wang, "Analysis and enhancement of incremental-quantity-based distance protection with grid-forming inverters," arXiv preprint arXiv:2604.10129, 2026.

[13] J. Wang, Y. Li, M. Tajdinian and M. T. Hoq, "New phase selection solution for distance protection with different system conditions," 19th IET Conference on Developments in Power System Protection (DPSP Europe 2025), Bilbao, Spain, 2025, pp. 217–221.

[14] B. Kasztenny, A. Guzman, N. Fischer, M. Mynam, D. Taylor, “Practical Setting Considerations for Protective Relays That Use Incremental Quantities and Traveling Waves” 2016, Available: https://selinc.com/api/download/117051/.

[15] T. Russell, P. Bhattarai, M. Cox, M. Quinteros, and T. Field, “Implementation and analysis of a digital model of the incremental-quantity distance element using EMTP” in 2023 76th Annual Conference for Protective Relay Engineers.